Space Flight Qualification on a Multi-Fiber Ribbon Cable and Array Connector Assembly

Xiaodan (Linda) Jin[a], Melanie N. Ott[b], Frank V. LaRocca[d], Ronald M. Baker[c], Bianca E. N. Keeler[c], Patricia R. Friedberg[b], Richard F. Chuska[d], Mary C. Malenab[a], Shawn L. Macmurphy[d]

[a]QSS Groups, Inc., 4500 Forbes Boulevard, Lanham, MD 20706
[b]NASA Goddard Space Flight Center, Code 562, Greenbelt MD 20771
[c]Sandia National Laboratories, Albuquerque, NM 87185
[d]MEI Technologies, 7404 Executive Place, Suite 500, Seabrook, MD, 20706

ABSTRACT

NASA's Goddard Space Flight Center (GSFC) cooperatively with Sandia National Laboratories completed a series of tests on three separate configurations of multi-fiber ribbon cable and MTP connector assemblies. These tests simulate the aging process of components during launch and long-term space environmental exposure. The multi-fiber ribbon cable assembly was constructed of non-outgassing materials, with radiation-hardened, graded index 100/140-micron optical fiber. The results of this characterization presented here include vibration testing, thermal vacuum monitoring, and extended radiation exposure testing data.

Keywords: multi-fiber, environmental, qualification, radiation, thermal, vibration

1. BACKGROUND

The results presented here are from qualification tests preformed on a multi-fiber ribbon cable equipped with MTP array connectors for Sandia National Laboratories. This test is the third set of testing conducted in this manner by the Photonics Laboratory (Code 562) at GSFC [1,2]. A similar test was conducted in the late 1990's of a multi-fiber ribbon cable MTP connectorized assembly, which was slated for use with the Fiber Optic Data Bus (FODB). This assembly, even though exposed to numerous environmental testing parameters, seemed to perform beyond expectations. Sandia National Laboratories selected a radiation hardened, 100/140 graded index fiber for their application. The fiber was manufactured by Nufern, located in East Granby, CT, and subsequently cabled into a ruggedized multi-fiber ribbon cable by W.L. Gore & Associates located in Newark, DE. The cable configuration included an ePTFE binder, aramid fiber strength member, and a kynar jacket. The cable was "preconditioned" before use, using a thermal cycling treatment, to prevent any possible shrinkage or deformation before termination procedures were applied. USCONEC, located in Hickory, North Carolina, manufactured the MTP connectors, non-outgassing connector components, and fabricated termini in both MTP and MT configurations. Each connector was assembled with a non-outgassing strain relief and ferrule boots using space flight procedures in compliance with NASA-STD-8739.5. The qualification test plan was designed to replicate the aging process during the mission. The results of this characterization included vibration testing, thermal vacuum monitoring, and extended radiation exposure testing.

2. FIBER CABLE CONFIGURATIONS

Three different configurations are defined in Table 1 and Figure 1(a,b,c). Configuration A is a single run cable with MTP connector terminated on both ends. Configuration B consisted of a single run cable that included mid-point MT ferrule terminations. Configuration C is terminated with MTP connector on both ends and mid-point fiber crossover circuit.

Table 1: Qualification Cable Configurations

Configuration	Length"	Description	MT Ferrule Ch Monitored
A	236	Single Run	1, 9
B	250	Single Run with Mid-Point Terminations	4, 12
C	24	Fiber Cross-Over Circuit	2, 11

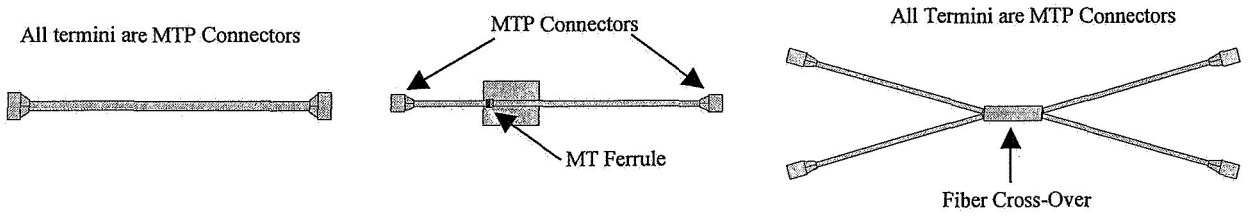

(a) Config. A **(b) Config. B** **(c) Config. C**

Figure 1(a,b,c): Qualification Cable Configurations

3. RANDOM VIBRATION CHARACTERZATION

To simulate launch conditions for component reliability, random vibration testing was conducted on the MTP cable assemblies. Pre-test insertion loss measurements were obtained to establish the performance baseline for each cable. A sample size of three cables each for configurations B and C, were used to collect active measurements during the vibration launch simulation. Two channels on each cable were actively monitored. Testing was performed on x, y, and z axes for a total of 3 minutes on each axis. Overall profile totaled 12.78grms.

Table 2: Vibration Profile

Frequency (Hz)	Level (Protoflight)
20	0.03140 g^2/Hz
70	0.48150 g^2/Hz
140	0.48150 g^2/Hz
150	0.25100 g^2/Hz
300	0.25100 g^2/Hz
400	0.10000 g^2/Hz
600	0.10000 g^2/Hz
2000	0.00900 g^2/Hz
Overall	12.78 g^2/Hz

3.1 Vibration setup specifications

A closed-loop feedback loop, including an accelerometer on the vibration fixture, is used to control the apparatus. Channels 4 and 12 of configuration B and channels 2 and 11 of configuration C were actively monitored. The optical test setup consisted of a RiFocs model 257L Dual LED source at a wavelength of 850nm, coupled into a 1 x 12 100/140um optical coupler as shown in Figure 2. The coupler was then mated to the fan-out reference cable, which is in-turn mated to the cable under test via an adapter. The above setup was securely mounted to the vibration assembly, which in turn was connected to the Agilent 8166A multi-channel optical power meter. A laptop computer utilizing LabVIEW data acquisition software recorded the cable-under-test optical transmission at 12 data points per second and monitored the 850nm optical source. All of the data was imported into an Excel spreadsheet for analysis. LED power measurement variations were subtracted from the collected data.

3.2 Cable Configurations:

3.2.1 Configuration B

Configuration B consisted of a single run, ribbonized, and ruggedized cable that included the MT mid-point terminations as shown in Figure 1(b). Each end of the configuration B cable was terminated MTP connector. At mid-point a custom ferrule adapter, developed by Sandia National Laboratories, mated the MT ferrules together. Sandia National Laboratories also fabricated the custom fixture so that the ferrule adapter could be secured on any of the three axes. The custom fixture was developed as a mounting point for the ferrule adapter and was tested to ensure NO resonant responses existed in the testing frequency range of 20 to 2000kHz. Two specific test methods were developed for the configuration B cable. One method was to test the MTP connectors and the other was to test the MT ferrule adapter. Figure 3(a) illustrates how the MTP adapter was mounted on the z-axis of the random vibration simulator. The lead MTP connector, mated to the source, was secured to the vibration table. The ferrule adapter along with the trail MTP connector, mated to the power meter, was located off the vibration table. Figure 3(b) illustrates how the MT ferrule adapter was mounted on the z-axis. Both the lead and trail MTP connectors were mated in the same fashion as the above mentioned. Through out the testing the active fiber channels 4 and 12 were monitored by an optical power meter at each axis.

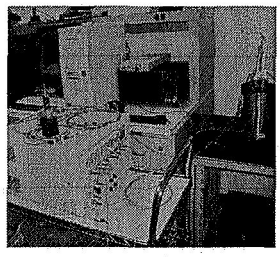

Figure 2

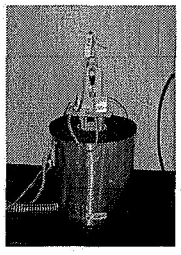

Figure 3 (a)

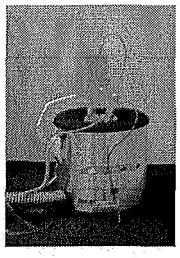

Figure 3 (b)

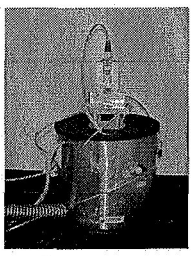

Figure 3 (c)

Figure 2 & 3(a,b,c): Vibration Test Setup; (a) Configuration B MTP Connector, (b) Configuration B Custom Ferrule Adapter, (c) Configuration C MTP Connector

3.2.2 Configuration C

Configuration C represents an fiber cross-over circuit. In this case, both the MTP connector and cross-over zone of the cable were tested. The MTP connector was mated to the reference cable, via an adapter, and both the connector and the cross-over region were secured to the vibration fixture (Refer to Figure 3c). This configuration was tested on x, y, and z axes for the durations mentioned previously.. Fiber channels 2 and 11 were actively monitored during testing.

4. VIBRATION RESULTS

Table 3 concentrates on the maximum change in optical transmission for channels 4 and 12 of configuration B and channels 2 and 11 for configuration C on each axis. With the exception of two measurements, all changes in optical transmission were within the 0.5dB specification limit. The LED source noise power drift, which never exceeded 0.03dB at any one time, was subtracted from the overall data. Table 4 shows the pre- and post-test comparison of insertion loss for each cable. Some cables show improved performance, which is likely due to improved fiber alignment between mated connector pairs. After each axis of the vibration test was completed, all optical fiber connections were inspected for apparent visual damage. Upon inspection, a cable from the configuration B developed some "pits" around the core on both of the MT ferrule terminations (refer to Figures 4 and 5). This was likely occurred during installation into the adapter and contaminated by some dirt. Unfortunately, this channel was not actively monitored during the testing. As a result this particular channel was closely monitored during the thermal vacuum testing. However, later verification proved that insertion loss did not change much between these two particular connections and no other cable connections were damaged during the vibration testing.

Table 3: Maximum Change in Optical Transmission at Each Axis

Cable ID#	Vib-axis	Ch#12	Ch#4	Ch#2	Ch#11
Configuration B-1, MTP	X	0.03	0.03		
	Y	0.02	0.02		
	Z	0.05	0.14		
Configuration B-1, MT	X	0.17	0.43		
	Y	0.15	0.3		
	Z	0.12	0.14		
Configuration B-2, MTP	X	0.04	0.02		
	Y	***0.61***	0.37		
	Z	0.04	0.02		
Configuration B-2, MT	X	0.11	***0.56***		
	Y	0.14	0.23		
	Z	0.1	0.14		
Configuration B-3, MTP	X	0.07	0.04		
	Y	0.04	0.02		
	Z	0.05	0.03		
Configuration C-1	X			0.01	0.04
	Y			0.02	0.05
	Z			0.12	0.04
Configuration C-2	X			0.04	0.05
	Y			0.03	0.05
	Z			0.1	0.1
Configuration C-3	X			0.02	0.03
	Y			0.08	0.04
	Z			0.2	0.06

Table 4: Insertion Losses Before and After Vibration

Cable ID#	Terminations	Ch#4	Ch#12	Ch#2	Ch#11
Configuration B-1	MTP	0.19	0.14		
	MT-1	-0.14	-0.39		
	MT-2	-0.32	0		
Configuration B-2	MTP	-0.08	0		
	MT-1	-0.45	-0.21		
	MT-2	0.05	-0.37		
Configuration B-3	MTP	0.07	0.28		
Configuration C-1	MTP-1			0.01	0.06
	MTP-2			0.01	0.08
	MTP-3			0.03	0.08
	MTP-4			0.02	0.08
Configuration C-2	MTP-1			-0.41	-0.32
	MTP-2			0.03	0.03
	MTP-3			0.03	0.11
	MTP-4			0.01	0.07
Configuration C-3	MTP-1			0.03	0.1
	MTP-2			0.05	0.11
	MTP-3			0.03	0.1
	MTP-4			0.05	0.11

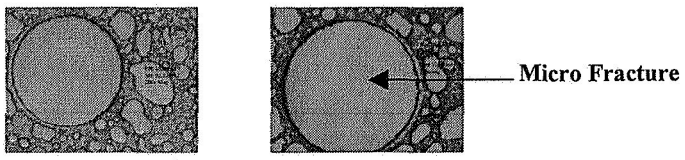

Figure 4: Image Inspection Before and After Vibration of Cable Config-B-1

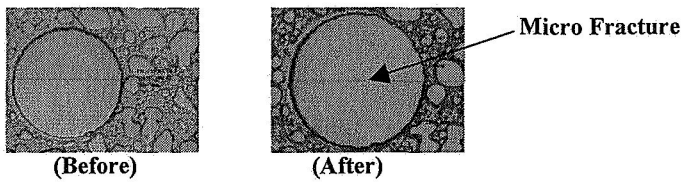

Figure 5: Image Inspection Before and After Vibration of Cable Config-B-1 (mid)

Table 5: Insertion Loss Measurement Before and After Vibration

Cable ID#	Ch#	Pre-vib	Post-vib	Δ (IL)
Configuration B-1, MT	2	0.65	0.44	-0.21
Configuration B-1, MT	2	0.41	0.26	-0.15

5. THERMAL VACUUM CHRACTERZATION

The MTP ribbon flight cables were exposed to thermal vacuum conditions. All three configurations, a combined total of fourteen cables, were placed inside the thermal vacuum chamber with the customized vacuum feed through ports. Two cables of each configuration were tested actively with two of each B and C configuration tested passively.

5.1 Thermal Vacuum Test Setup

One assembly, using a fan-out style cable, was the input connecting the MTP qualification cables to the LED source. The other side was the output of the MTP qualification cable connected to the Agilent 8166A power meter. The same LED source used in the vibration testing was also used with the thermal vacuum testing. Optical transmissions on channels 1 and 9 of configuration A, channels 4 and 12 of configuration B, and channels 2 and 11 of configuration C were actively monitored. Due to the concern of some end-face damage resulting from the vibration testing, channels 2 and 4 of configuration B were also be monitored during testing. Thermal vacuum testing setup consisted of 60 total thermal cycles, -25°C to 80°C, ramp rate of 1°C/min, and 30 minutes dwell time at each extreme, and vacuum pressure in the range of 10^{-6} to 10^{-8} torr. The LED source was coupled into optical reference cables, which in turn connected to the MTP fan-out cables feed through the test portals inside the thermal vacuum chamber. The outputs of the MTP fan-out cables were connected to the Agilent 8166A power meter for observation. Using two different laptops equipped with LabVIEW data acquisition software and hardware, optical transmission changes, thermal temperature, and chamber pressure were recorded.

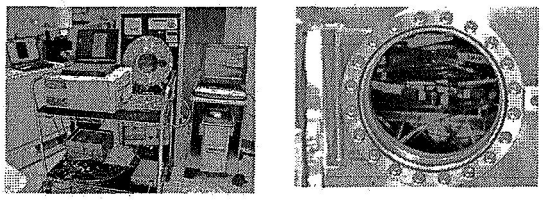

Figure 6 & 7: Thermal Vacuum Setup and Cables Inside Chamber

6. THERMAL RESULTS

Table 6 represents the thermal induced optical transmission changes with the LED source power shift subtracted. This calculation was made so only thermal induced optical transmission changes are represented. The third column of Table 6 shows the maximum optical transmission power changes for a single cycle and the last column of Table 6 represents total optical transmission changes over the entire 60 cycles of testing. As stated earlier, the concern for the damaged channel 2 of configuration B passed the thermal vacuum testing without any problem. Once the thermal testing was completed an inspection of all end-face connectors was conducted. The inspection showed no connectors were damaged during thermal vacuum testing.

Table 6: Thermal Induced Optical Transmission Changes

Cable ID#	Ch#	Max. Change within a cycle	Max. Change over entire test duration
Configuration A-1	1	0.8	1.1
	9	0.5	0.7
Configuration A-2	1	0.7	1.0
	9	0.7	1.0
Configuration B-1	2	1.5	1.6
	4	0.4	0.7
Configuration B-2	4	1.0	1.6
	12	1.5	1.9
Configuration C-1	2	0.4	0.5
	11	0.2	0.2
Configuration C-2	2	0.5	0.8
	11	0.3	0.4

7. RADIATION CHRACTERZATION

To simulate a space flight environment, a gamma (Cobalt 60) radiation chamber was used for testing the MTP assemblies for radiation induced dosing. The radiation chamber selected for this portion of the testing is located at NASA Goddard Space Flight Center. Two cables from configurations A and C were selected for gamma radiation exposure at two discrete dose rates. Each of the selected cables was placed inside a thermal chamber oven maintaining a cold temperature of –25°C for an uninterrupted extended period of time.

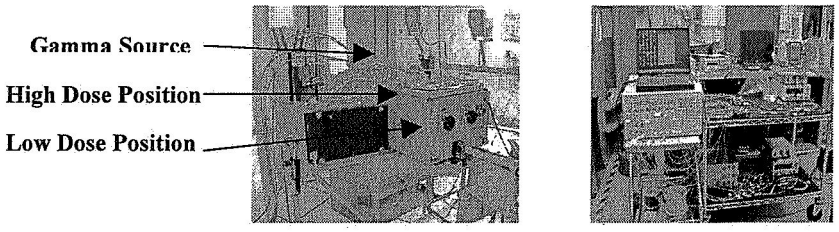

Figure 8 & 9: Show Thermal Chamber Positioned in Front of Radiation Source and Test Setup

7.1 Radiation Test Setup

One set of optical cables from configuration A and C were mounted on the front door inside the thermal chamber. This was done to achieve a high dose rate of ~120rads/min. The other set of optical cables were mounted on a custom fabricated aluminum plate orientated to face the rear portion of the chamber in order to achieve ~12rads/min. In order to monitor the equipment inside the gamma radiation chamber properly, 20m reference cables were used to connect

cables under test to Agilent 8166A power meter and the optical power sources. Figure 8 shows how the thermal chamber was oriented in front of the gamma radiation source. The reference fan-out cables were mounted on top of the thermal chamber, shielded behind lead bricks, out of direct beam exposure. Figure 9 shows the testing setup used to monitor the radiation effects. This setup is similar to the vibration and thermal vacuum testing setup conducted previously, except the input optical power was attenuated to less then 1uW CW at 850nm to limit photo-bleaching. Measurements were captured every 1-minute with the test actually beginning a few minutes before radiation began in order to capture initial dose data. The LED source was monitored during the duration of the test and the power drift was subtracted out of the final calculation.

7.2 Radiation testing results:

Table 8 summarizes the total dose, total dose rate, and testing results for each cable. The radiation testing was conducted inside a thermal chamber oven at –25°C for approximately 385 hours, and then for an additional 48 hours at the room temperature. Once the radiation portion was completed the experiment was relocated to the Photonics lab and testing continued to gather additional recovery data during the annealing process. The objective for this test was to expose the cables simultaneously to two different dose rates inside the thermal chamber at a single temperature. However, testing showed quite early on the temperature on the back of the thermal chamber started to get colder then what was reported at the front of the chamber. This was directly related to ice build up on the back portion of the thermal chamber causing a significant drop in temperature. In order to try and correct this problem a purge of nitrogen gas was feed into the chamber during testing to prevent further ice build up. Through the entire test the temperature in the back of the thermal chamber was roughly –33°C, slightly colder than expected, and the front portion of the thermal chamber was roughly –21°C, slightly warmer then expected target rates. The reference fan-out cables, used to connect the LED source and Optical Power Meter, had to be fed through the thermal chamber feed-through holes in order to be mated to the cables under test. This left a significant portion of reference cable exposed to the gamma radiation, which may have caused data inaccuracy of the shorter assemblies.

Table 8: Radiation Testing Parameters and Results

Cable ID	Ch#	Dose rate (rads/ min)	Total dose (Krad)	Cable Length	Cold Temp	Attenuation at cold temp	Attenuation at room temp of 24C	Attenuation after anneal for 7 days
Config. A-2,	1	12	244	6.35m	-33C	2.3 dB/m	1.9 dB/m	1.4 dB/m
	9	12	244	6.35m	-33C	2.4 dB/m	1.9 dB/m	1.4 dB/m
Config. A-1	1	120	2440	6.35m	-21C	2.1 dB/m	1.9 dB/m	1.5 dB/m
	9	120	2440	6.35m	-21C	2.1 dB/m	2.0 dB/m	1.6 dB/m
Config. C-4	2	12	244	0.61m	-33C	22.1 dB/m	19.2 dB/m	14.9 dB/m
	11	12	244	0.61m	-33C	21.6 dB/m	18.9 dB/m	14.3 dB/m
Config. C-3	2	120	2440	0.61m	-21C	21.1 dB/m	19.2 dB/m	14.9 dB/m
	11	120	2440	0.61m	-21C	20.8 dB/m	19.0 dB/m	14.3 dB/m

Figure 10 represents radiation-induced attenuation for chan#9 cable configuration A at two different dose rates. As expected, at the beginning of the test, the high dose rate data curve shows slightly higher radiation induced attenuation than low dose rate. Later, as the temperature on the low dose rate cable was getting much colder, the attenuation on low dose rate was getting higher than high dose rate. At the end of the thermal portion of the testing, the thermal chamber returned to room temperature and the fiber was still exposed to the radiation for another two days. The fiber began to saturate and the low dose rate finally showed lower attenuation than high dose rate. After another seven days annealing process for recovery the low dose rate showed much lower attenuation than high dose rate.

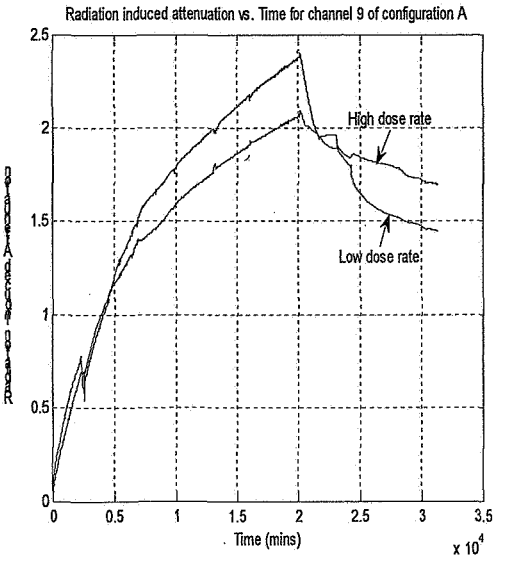

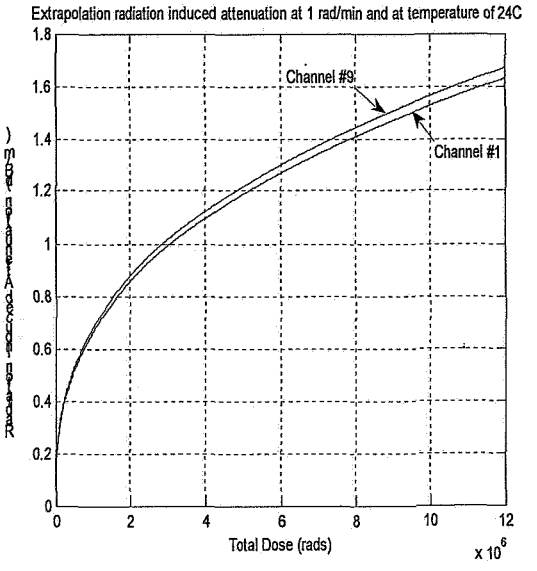

Figure 10: Complete Data Curve of Radiation-Induced Attenuation for Ch9 Configuration A

Figure 11: Extrapolation Curve at the Dose Rate of 1 rads/min up to 12 Mrads at Temperature of 24°C

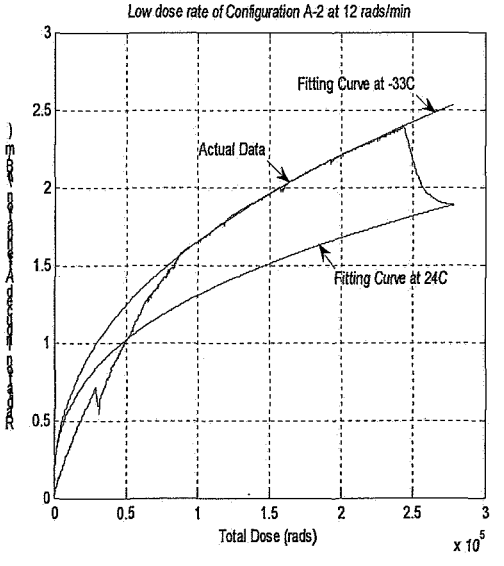

(a)

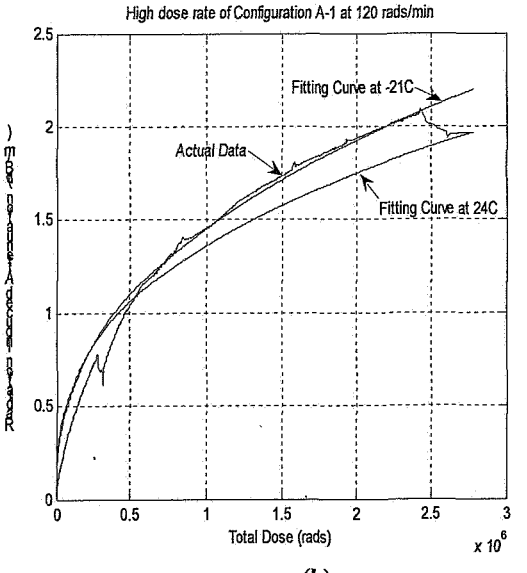

(b)

Figure 12: Cable Configuration A Radiation-Induced Attenuation Data
a) At 120 rads/min exposure with curve fit, and b) at 12 rads/min exposure with curve fit

Mathematical data processing software called MatLab was used to process the collected data. The Friebele Model was chosen as the extrapolation method [4]. Using this extrapolation method, the equation for radiation-induced attenuation in optical fiber takes the form:

$$A(D)=C_0\phi^{1-f}D^f \quad (1)$$

A (D) is the radiation induced attenuation, D is the total dose, ϕ is the dose rate, C_0 is a constant, and f is a constant less than one. The radiation test on channel 9, of cable configuration A-1, saw a high dose rate of 120 rads/min which translates to A (D)=5.4 x $10^{-3}D^{.4052}$(dB/m) with a curve temperature fit of –21°C. Channel 9 configuration A-2 saw a low dose rate of 12 rads/min which translates to A (D)=1.36 x 10^{-2} $D^{.4169}$ (dB/m) with a curve temperature fit of –33°C. Based upon the model equation (1) no general model can be derived without making some assumptions about the constants C_0 and f [2,3]. Two sets of data are necessary to determine which C_0 and f should be used for extrapolation to other dose rates at different temperatures. Under the assumption that f is a linear function of temperature T and C_0 is a linear function of dose rate ϕ, the general model for other dose rates and other temperatures can be made using two data sets. Solving for f (T) using both data sets, the expression is

$$f(T) = -9.75 \times 10^{-4}T + 0.3847 \quad (2)$$

At room temperature of 24°C, f = 0.3613. Using the same f in the curve fitting to both data sets at room temperature of 24°C as shown in Figure 10, $C_0 = 0.43 \times 10^{-3}$ at 120 rads/min and $C_0 = 4.2 \times 10^{-3}$ at 12 rads/min. Solving for $C_0(\phi)$ using both data sets, the expression is

$$C_0(\phi) = -3.49 \times 10^{-5}\phi + 4.62 \times 10^{-3} \quad (3)$$

Using equation (3), dose rate becomes very small or less than 1 rad/min which is typical of space flight background radiation, C_0 becomes 4.6×10^{-3}, independent of dose rate. Under this assumption that most space flight environments have background radiation at levels less than 1 rad/min, the expression for radiation-induced attenuation at room temperature of 24C can be described as:

$$A(D) = 4.62 \times 10^{-3}\phi^{1-0.3613} D^{0.3613} \quad (4)$$

Equation (4) represents the extrapolation model equation derived from channel 9 of the two cable sets. Using the same constant of f = 0.3613 on channel 1 of two cables, the extrapolation model equation was derived and described as:

$$A(D) = 4.51 \times 10^{-3}\phi^{1-0.3613} D^{0.3613} \quad (5)$$

Figure 11 shows the extrapolated data for 1 rad/min up to 12 Mrads using the extrapolation model equations for channel 1 and 9, and the estimated radiation induced attenuation at 12 Mrads is 1.63dB/m for channel 1 and 1.67dB/m for channel 9. As mentioned before, a small portion of reference fan-out cable was pulled inside the chamber, adding more loss to the testing results, so the extrapolated data represents the worse case scenario and gives a higher loss than would be expected.

The radiation test is actually to test the darkening effect of the fiber itself in the radiation environments. In order to achieve more accurate data, longer fiber of about 100m is recommended for the test. The lessons learned from this testing are: (1) use two separate thermal chambers to run two different dose rate experiments so not have the temperature difference problem due to the ice build up. (2) Do not leave the reference fan-out cables inside the thermal chamber. This minimizes the data accuracy uncertainty.

8. CONCLUSION

A Multi-fiber ribbon cable assembly equipped with MTP array connectors was characterized for a space flight environmental use for Sandia National Laboratories. Three distinctively different configurations of ribbon cable were tested and characterized by three tests: vibration testing, thermal vacuum performance, and radiation exposure.

During vibration testing, two channels of each cable were actively monitored at three different axes. Each of these axes tested for three minutes. Two specific test approaches were used to test configuration B's MTP connector and MT ferrule adapter. A total forty-eight tests were conducted (two channels on each cable). From the collected data points, only two data points were just above the specification of 0.5dB. All optical fiber end faces were visually inspected for any damage after each axis vibration testing. One channel of one MT mating connector exhibited signs of damage to its end-face, but later verified to show no interruption during the thermal vacuum testing. Thermal cycling and vacuum testing was conducted on all cables. Two of the B and C configurations were tested actively and two were tested passively for total of 60 thermal cycles. The collected data shows that all channels exhibited less then 2dB of the maximum optical power change. Again, all the insertion loss measurements and fiber end-face visual inspections were made before and after the thermal vacuum test, and no fiber end-face was found damaged.

Radiation exposure testing proved most challenging. Two sets of configuration A and one set of configuration C were exposed to high dose rates and low dose rates of gamma radiation. Because configuration C's cable was too short, the focus was on the longer cable (6.35m) of configuration A. Just before the thermal chamber was turned off, the recorded radiation induced attenuation was 2.4dB/m for the low dose rate, and 2.1dB/m for the high dose rate. After the temperature returned to room temperature, the recorded radiation induced attenuation for both dose rates were 1.9dB/m. Most space flight environments have background radiation at levels less than 1 rad/min, the extrapolated data for 1 rad/min up to 12 Mrads at room temperature was given. Further testing with a longer reference cable ($\geq$100m) might be necessary to achieve more accurate results and extrapolation model for this type of fiber.

ACKNOWLEDGMENT

The Photonics Lab (GSFC) would like to acknowledge Sandia National Laboratories for funding this work. Also, special thanks to Steve Brown and Eugene Gerashchenko of the radiation facility group at NASA GSFC for support in this effort.

REFERENCES

1. Melanie N. Ott, Joy W. Bretthauer, "Twelve channel optical fiber connector assembly: from commercial off the shelf to space flight use," Photonics For Space Environments VI, Proceedings of SPIE Vol. 3440, 1998.
2. Melanie N. Ott, Shawn Macmurphy, and Pat Friedberg, "Characterization of a twelve channel optical fiber, ribbon cable and MTP array connector assembly for space flight environments," International Society for Optical Engineering, SPIE Aerosense Conference Proceedings on Enabling Photonic Technologies for Aerospace and Applications IV, Vol. 4732, April 2002.
3. Melanie N. Ott, "Fiber Optic Cable Assemblies for Space Flight II: Thermal and Radiation Effects," Photonics For Space Environments VI, Proceedings of SPIE Vol. 3440, 1998.
4. E. J. Friebele, M.E. Gingerich, D. L. Griscom, "Extrapolating Radiation-Induced Loss Measurements in Optical Fibers from the Laboratory to Real World Environments", 4th Biennial Department of Defense Fiber Optics and Photonics Conference, March 22-24, 1994.